

Gluon Pseudo-Distributions at Short Distances: Forward Case

Ian Balitsky, Wayne Morris and Anatoly Radyushkin

Physics Department, Old Dominion University, Norfolk, VA 23529, USA

Thomas Jefferson National Accelerator Facility, Newport News, VA 23606, USA

Abstract

We present the results that are necessary in the ongoing lattice calculations of the gluon parton distribution functions (PDFs) within the pseudo-PDF approach. We give a classification of possible two-gluon correlator functions and identify those that contain the invariant amplitude determining the gluon PDF in the light-cone $z^2 \rightarrow 0$ limit. One-loop calculations have been performed in the coordinate representation and in an explicitly gauge-invariant form. We made an effort to separate ultraviolet (UV) and infrared (IR) sources of the $\ln(-z^2)$ -dependence at short distances z^2 . The UV terms cancel in the reduced Ioffe-time distribution (ITD), and we obtain the matching relation between the reduced ITD and the light-cone ITD. Using a kernel form, we get a direct connection between lattice data for the reduced ITD and the normalized gluon PDF. We also show that our results may be used for a rather straightforward calculation of the one-loop matching relations for quasi-PDFs.

1. Introduction

Lattice calculations of parton distribution functions (PDFs) are now a subject of considerable interest and efforts (see Ref. [1] for a recent review and references to extensive literature). Modern efforts aim at the extractions of PDFs $f(x)$ themselves rather than their x^N moments. On the lattice, this may be achieved by switching from local operators to current-current correlators [2]. A further idea is to start with equal-time correlators [3].

X. Ji, in the paper [4] that strongly stimulated further development, made a ground-breaking proposal to consider equal-time versions of nonlocal operators defining PDFs, distribution amplitudes, generalized parton distributions, and transverse momentum dependent distributions. In the case of usual PDFs, the basic concept of Ji's approach is a "parton quasi-distribution" (quasi-PDF) $Q(y, p_3)$ [4, 5], and PDFs are obtained from the large-momentum $p_3 \rightarrow \infty$ limit of quasi-PDFs.

Other approaches, such as the "good lattice cross sections" [6, 7], the Ioffe-time analysis of equal-time correlators [3, 8, 9] and the pseudo-PDF approach [10, 11, 12] are coordinate-space oriented, and extract parton distributions taking the short-distance $z_3 \rightarrow 0$ limit.

Both the $p_3 \rightarrow \infty$ and $z_3 \rightarrow 0$ limits are singular, and one needs to use *matching relations* to convert the Euclidean lattice data into the usual light-cone PDFs. In the quasi-PDF approach, such relations were studied for quark [4, 13, 14, 15] and gluon PDFs [16, 17, 18], for the pion distribution amplitude (DA) [19] and generalized parton distributions (GPDs) [19, 20, 21].

Within the pseudo-PDF approach, the matching relations were derived for non-singlet PDFs [22, 23, 24, 25,

15]. The strategy of the lattice extraction of non-singlet GPDs and the pion DA using the pseudo-PDF methods was outlined in a recent paper Ref. [26], where the matching conditions for these cases have been also derived. In the present paper, our main goal is to describe the basic points of the pseudo-PDF approach to extraction of unpolarized gluon PDFs, and also to find one-loop matching conditions.

In the gluon case, the calculation is complicated by strict requirements of gauge invariance. In this situation, a very effective method is provided by the coordinate-representation approach of Ref. [27]. It is based on the background-field method and the heat-kernel expansion. It allows, starting with the original gauge-invariant bilocal operator, to find its modification by one-loop corrections. The results are obtained in an explicitly gauge-invariant form.

In this approach, there is no need to specify the nature of matrix element characteristic of a particular parton distribution. This means that one and the same Feynman diagram calculation may be used both for finding matching conditions for PDFs (given by forward matrix elements), and for DA's and GPDs corresponding to non-forward ones (see Ref. [26] for an illustration of how this works for quark operators).

The paper is organized as follows. In Section 2, we analyze the kinematic structure of the matrix elements of the gluonic bilocal operators, and identify those that contain information about the twist-2 gluon PDF.

Next, we discuss one-loop corrections. In Section 3, we analyze the gauge-link self-energy contribution and specific properties of its ultraviolet and short-distance behavior. Our results for the vertex corrections to the gluon link are given in Section 4 in the form that is valid both in forward and non-forward cases. The "box" dia-

gram is discussed in Section 5. Since our results in this case are rather lengthy, we present just some of them, and in the forward case only. The gluon self-energy corrections are discussed in Section 6.

The subject of Section 7 is the structure of perturbative evolution of the gluon operators and matching conditions. Section 8 contains a summary of the paper.

2. Matrix elements

The nucleon spin-averaged matrix elements for operators composed of two-gluon-fields (with all four indices non-contracted) are specified by

$$M_{\mu\alpha;\lambda\beta}(z, p) \equiv \langle p | G_{\mu\alpha}(z) G_{\lambda\beta}(0) | p \rangle, \quad (2.1)$$

where $[z, 0]$ is the standard straight-line gauge link in the gluon (adjoint) representation

$$[x, y] \equiv \text{Pexp} \left\{ ig \int_0^1 dt (x-y)^\mu \tilde{A}_\mu(tx + (1-t)y) \right\}. \quad (2.2)$$

The tensor structures for a decomposition over invariant amplitudes may be built from two available 4-vectors p_α, z_α and the metric tensor $g_{\alpha\beta}$. Incorporating the antisymmetry of $G_{\rho\sigma}$ with respect to its indices, we have

$$\begin{aligned} M_{\mu\alpha;\lambda\beta}(z, p) = & \\ & (g_{\mu\lambda} p_\alpha p_\beta - g_{\mu\beta} p_\alpha p_\lambda - g_{\alpha\lambda} p_\mu p_\beta + g_{\alpha\beta} p_\mu p_\lambda) \mathcal{M}_{pp} \\ & + (g_{\mu\lambda} z_\alpha z_\beta - g_{\mu\beta} z_\alpha z_\lambda - g_{\alpha\lambda} z_\mu z_\beta + g_{\alpha\beta} z_\mu z_\lambda) \mathcal{M}_{zz} \\ & + (g_{\mu\lambda} z_\alpha p_\beta - g_{\mu\beta} z_\alpha p_\lambda - g_{\alpha\lambda} z_\mu p_\beta + g_{\alpha\beta} z_\mu p_\lambda) \mathcal{M}_{zp} \\ & + (g_{\mu\lambda} p_\alpha z_\beta - g_{\mu\beta} p_\alpha z_\lambda - g_{\alpha\lambda} p_\mu z_\beta + g_{\alpha\beta} p_\mu z_\lambda) \mathcal{M}_{pz} \\ & + (p_\mu z_\alpha - p_\alpha z_\mu) (p_\lambda z_\beta - p_\beta z_\lambda) \mathcal{M}_{ppzz} \\ & + (g_{\mu\lambda} g_{\alpha\beta} - g_{\mu\beta} g_{\alpha\lambda}) \mathcal{M}_{gg}, \end{aligned} \quad (2.3)$$

where the amplitudes \mathcal{M} are functions of the invariant interval z^2 and the Ioffe time [28] $(pz) \equiv -\nu$ (the minus sign is introduced for further convenience).

Since the matrix element should be symmetric with respect to interchange of the fields (which amounts to $\{\mu\alpha\} \leftrightarrow \{\lambda\beta\}$ and $z \rightarrow -z$), the functions \mathcal{M}_{pp} , \mathcal{M}_{zz} , \mathcal{M}_{gg} , \mathcal{M}_{ppzz} and $\mathcal{M}_{pz} - \mathcal{M}_{zp}$ are even functions of ν , while $\mathcal{M}_{pz} + \mathcal{M}_{zp}$ is odd in ν .

The usual light-cone gluon distribution is obtained from $g^{\alpha\beta} M_{+\alpha;\beta+}(z, p)$, with z taken in the light-cone ‘‘minus’’ direction, $z = z_-$. We have

$$g^{\alpha\beta} M_{+\alpha;\beta+}(z_-, p) = -2p_+^2 \mathcal{M}_{pp}(\nu, 0), \quad (2.4)$$

i.e., the PDF is determined by the \mathcal{M}_{pp} structure,

$$-\mathcal{M}_{pp}(\nu, 0) = \frac{1}{2} \int_{-1}^1 dx e^{-ix\nu} x f_g(x). \quad (2.5)$$

Thus, we should choose the operators with the sets $\{\mu\alpha; \lambda\beta\}$ that contain \mathcal{M}_{pp} in their parametrization.

Note that it is the density of the momentum $G(x) \equiv x f_g(x)$ carried by the gluons rather than their number density $f_g(x)$ that is a natural quantity in this definition of the gluon PDF. In the local $z_- = 0$ (or $\nu = 0$) limit, the x -integral gives the fraction of the hadron’s plus momentum carried by the gluons. In the absence of gluon-quark transitions, this fraction is conserved, which puts a restriction on the gg -component of the Altarelli-Parisi [29] kernel. Namely, it should have the plus-prescription property when applied to $G(x)$.

Due to antisymmetry of $G_{\rho\sigma}$ with respect to its indices, the values $\alpha = +$ and $\beta = +$ are excluded from the summation in Eq. (2.4). Furthermore, since $g_{--} = 0$, the combination $g^{\alpha\beta} M_{+\alpha;\beta+}(z, p)$ includes only summation over transverse indices $i, j = 1, 2$, i.e. reduces to $g^{ij} M_{+i;j+}(z, p) \equiv M_{+i;+i}(z, p)$ (we switched here to Euclidean summation over i), for which we have

$$M_{+i;+i} = M_{0i;0i} + M_{3i;3i} + (M_{0i;3i} + M_{3i;0i}). \quad (2.6)$$

In the local $z_3 = 0$ limit, these three combinations are proportional to \mathbf{E}_\perp^2 , \mathbf{B}_\perp^2 and the third component $(\mathbf{E} \times \mathbf{B})_3$ of the Poynting vector, respectively.

The decomposition of these combinations (with summation over i) in the basis of the \mathcal{M} structures is

$$M_{0i;0i} = 2p_0^2 \mathcal{M}_{pp} + 2\mathcal{M}_{gg}, \quad (2.7)$$

$$\begin{aligned} M_{3i;3i} = & 2p_3^2 \mathcal{M}_{pp} + 2z_3^2 \mathcal{M}_{zz} \\ & + 2z_3 p_3 (\mathcal{M}_{zp} + \mathcal{M}_{pz}) - 2\mathcal{M}_{gg}, \end{aligned} \quad (2.8)$$

$$M_{0i;3i} = 2p_0 (p_3 \mathcal{M}_{pp} + z_3 \mathcal{M}_{pz}), \quad (2.9)$$

$$M_{3i;0i} = 2p_0 (p_3 \mathcal{M}_{pp} + z_3 \mathcal{M}_{zp}). \quad (2.10)$$

All of them contain the \mathcal{M}_{pp} function defining the gluon distribution, though with different kinematical factors. Unfortunately, none of them is just \mathcal{M}_{pp} : they all contain contaminating terms. Moreover, the $M_{3i;3i}$ matrix element (proposed originally [4] for extractions of the gluon PDF on the lattice) contains three contaminations, while the others have just one addition. In particular, the matrix element $M_{0i;0i}$ has \mathcal{M}_{gg} as a contaminating term. It is easy to see that

$$M_{ji;j} \equiv \langle p | G_{ji}(z) G_{ij}(0) | p \rangle = -2\mathcal{M}_{gg}, \quad (2.11)$$

where the summation over both i and j is assumed. Hence, the combination

$$M_{0i;0i} + M_{ji;j} = 2p_0^2 \mathcal{M}_{pp} \quad (2.12)$$

may be used for extraction of the twist-2 function \mathcal{M}_{pp} .

Combining together matrix elements of different types, one should take into account that, off the light cone, these matrix elements have extra ultraviolet divergences related to presence of the gauge link. Due to the local nature of ultraviolet divergences, each matrix element, for any set of its indices $\{\mu\alpha; \lambda\beta\}$, is multiplicatively renormalizable with respect to these divergences [30]. However, choosing different sets of $\{\mu\alpha; \nu\beta\}$, we

get, in general, different anomalous dimensions.

Thus, it is not evident *a priori* which linear combinations of these matrix elements are multiplicatively renormalizable. In Ref. [31], it was established that the combinations represented in Eq. (2.6), namely, $M_{0i;i0}$, $M_{3i;i3}$, $M_{0i;i3} + M_{3i;i0}$ (and also $M_{0i;i3} - M_{3i;i0}$), with summation over transverse indices i , are each multiplicatively renormalizable at the one-loop level.

Furthermore, the combination $G_{ij}G_{ij}$ (with summation over transverse i, j) equals to $2G_{12}G_{12}$, whose matrix elements are multiplicatively renormalizable. As we will see, it has the same one-loop UV anomalous dimension as $M_{0i;i0}$, hence the combination of Eq. (2.12) is multiplicatively renormalizable at the one-loop level. A possible subject for further studies is to investigate if this is true in higher orders.

The combination $g^{\alpha\beta}M_{3\alpha;3\beta}$, containing a covariant summation over α and β , was also found to be multiplicatively renormalizable. It is given by

$$g^{\alpha\beta}M_{3\alpha;3\beta} = (2p_3^2 - m^2)M_{pp} + 3z_3^2M_{zz} + 3p_3z_3(M_{zp} + M_{pz}) + p_0^2z_3^2M_{ppzz} - 3M_{gg}, \quad (2.13)$$

and has the largest number (four) of contaminations.

The function $g^{\alpha\beta}M_{0\alpha;0\beta}$, also involving a covariant summation, was used in the first attempt [32] of the lattice extraction of the gluon PDF. However, as noted in Ref. [31], it is not multiplicatively renormalizable.

In any theory with a dimensionless coupling constant, the matrix elements $M(z, p)$ contain $\sim \ln(-z^2)$ terms corresponding to perturbative (or ‘‘DGLAP’’ for Dokshitzer-Gribov-Lipatov-Altarelli-Parisi [33, 29, 34]) evolution. One may wonder which combinations have a diagonal DGLAP evolution at one loop.

To answer these questions, we have calculated the modification of the original bilocal operator by one-loop gluon exchanges.

3. Link self-energy contribution and ultraviolet divergences

The simplest diagram corresponds to the self-energy correction for the gauge link (see Fig. 1). Its calculation is the same as in case of the quark bilocal operators (see, e.g., Ref. [23]). At one loop, one should just the change the color factor $C_F \rightarrow C_A$. Thus, we have

$$\Gamma_\Sigma(z) = (ig)^2 C_A \frac{1}{2} \int_0^1 dt_1 \int_0^1 dt_2 z^\mu z^\nu D_{\mu\nu}^c[z(t_2 - t_1)], \quad (3.1)$$

where $D_{\mu\nu}^c(z) = g_{\mu\nu}/4\pi^2 z^2$ is the Feynman-gauge gluon propagator in the coordinate representation. The resulting integrals over the link parameters t_1, t_2

$$\int_0^1 dt_1 \int_0^1 \frac{dt_2}{(t_2 - t_1)^2} \quad (3.2)$$

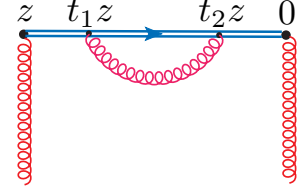


Figure 1: Self-energy-type correction for the gauge link.

diverge when $t_1 \sim t_2$, i.e., when the endpoints $t_1 z$ and $t_2 z$ of the gluon propagator are close to each other. So, one may suspect that this divergence has an ultraviolet origin. To see that this is the case, we use the dimensional regularization (DR) [35] in the UV region, switching to d dimensions. As a result, the gluon propagator in the coordinate space acquires an extra factor $(-z^2)^{2-d/2}$. This results in an extra $(t_2 - t_1)^{2-d/2}$ factor in Eq. (3.2), and the integral there converges for sufficiently small d .

To preserve gauge invariance, our calculations were made using massless gluons and the dimensional regularization. However, in the case of the link self-energy diagram, the use of DR (which is basically just a mathematical trick) is rather misleading in a couple of points.

The relevant subtleties may be illustrated by using the Polyakov prescription $1/z^2 \rightarrow 1/(z^2 - a^2)$ for the gluon propagator in the coordinate representation [36] (see also Refs. [37, 23]). It softens the gluon propagator at intervals $-z^2 \lesssim a^2$, and eliminates its singularity at $z^2 = 0$. In this respect, it is similar to the UV regularization produced by a finite lattice spacing, and gives

$$\Gamma_\Sigma(z, a) = -g^2 C_A \frac{z^2}{8\pi^2} \int_0^1 dt_1 \int_0^1 \frac{dt_2}{z^2(t_2 - t_1)^2 - a^2}. \quad (3.3)$$

The regularized integral vanishes on the light cone $z^2 = 0$ and converges for spacelike z . Taking $z = z_3$ and calculating the integrals gives [37, 23]

$$\Gamma_\Sigma(z_3, a) = -C_A \frac{\alpha_s}{2\pi} \left[2 \frac{z_3}{a} \tan^{-1}\left(\frac{z_3}{a}\right) - \ln\left(1 + \frac{z_3^2}{a^2}\right) \right]. \quad (3.4)$$

The result contains a linear $\sim 1/a$ divergence that is missed if one uses the DR. Furthermore, for a fixed a and small z_3 it behaves like z_3^3/a^2 , i.e., $\Gamma_\Sigma(z, a)$ vanishes for $z_3 = 0$, as expected: there is no link if $z_3 = 0$. It also vanishes on the light cone $z^2 = 0$.

The fact that $\Gamma_\Sigma(z_3 = 0, a) = 0$ means that, for a fixed a , this term gives no corrections to the local limit of the $G_{\mu\alpha}(z)[z, 0]G_{\lambda\beta}(0)$ operator, e.g., to the energy-momentum tensor (EMT). Since the matrix element of the EMT gives the fraction of the hadron momentum carried by the gluons, the link self-energy correction does not change this fraction. This is a natural phenomenon in the absence of the gluon-quark transitions.

However, if one formally takes the $a \rightarrow 0$ limit for a fixed z_3 in Eq. (3.4), then $\ln\left(1 + \frac{z_3^2}{a^2}\right)$ converts into

the expression $\ln(z_3^2/a^2)$ singular for $z_3 = 0$. Similarly, using the DR, one faces an outcome proportional to

$$(-z^2\mu_{\text{UV}}^2)^{\epsilon_{\text{UV}}}/\epsilon_{\text{UV}} = 1/\epsilon_{\text{UV}} + \ln(-z^2\mu_{\text{UV}}^2) + \dots, \quad (3.5)$$

where μ_{UV} is the scale accompanying this UV dimensional regularization. Again, the starting expression vanishes for $z^2 = 0$, but renormalizing it by a subtraction of the $1/\epsilon_{\text{UV}}$ pole, one may apparently conclude that, in addition to the UV divergence, this diagram contains a singularity on the light cone $z^2 = 0$.

For this reason, in our DR results we will explicitly separate the z^2 -dependence induced by the UV singular terms (that actually vanish on the light cone) and that present in the DGLAP-evolution logarithms $\ln(-z^2\mu_{\text{IR}}^2)$, where μ_{IR} is the scale associated with the DR regularization of the collinear singularities.

The main difference is that if, instead of DR, one regularizes collinear singularities by using a physical IR cut-off Λ (like nonzero gluon virtuality or gluon mass), the one-loop result, proportional to the modified Bessel function $K_0(\sqrt{-z^2}\Lambda^2)$, remains singular for $z^2 = 0$, unlike the UV-induced logarithm $\ln(1 - z^2/a^2)$.

In the case of the link self-energy diagram, we have UV singularities only. Its correction to the $G_{\mu\alpha}(z)G_{\lambda\beta}(0)$ operator is given by

$$-\frac{g^2 N_c}{4\pi^2 [(-z^2\mu_{\text{UV}}^2 + i\epsilon)]^{\frac{d}{2}-2}} \frac{\Gamma(d/2-1)}{(3-d)(4-d)} G_{\mu\alpha}(z)G_{\lambda\beta}(0), \quad (3.6)$$

where the $1/(3-d)(4-d)$ factor results from the integral

$$\int_0^1 dt_1 \int_0^{t_1} dt_2 (t_1 - t_2)^{2-d} = \frac{1}{(3-d)(4-d)}$$

produced by the DR of the gluon propagator $D^c(t_1 z - t_2 z)$. The pole for $d = 3$ ($d = 4$) corresponds to the linear (logarithmic) UV divergence in Eq. (3.4).

4. Vertex contributions

There are also vertex diagrams involving gluons that connect the gauge link with the gluon lines, see Fig. 2.

We use the method of calculation described in Ref. [27]. It is based on the background-field technique, with the gluon propagator taken in the ‘‘background-Feynman’’ (bF) gauge [27]. It should be noted that the three-gluon vertex in the bF gauge is different from the usual Yang-Mills vertex (see e.g. [38]). Therefore, the results obtained for separate diagrams in the bF gauge differ from those obtained in the usual Feynman gauge and only the sum of all diagrams must be the same.

4.1. UV divergent term

Clearly, the gluon exchange produces a correction just to one of the fields in the $G_{\mu\alpha}(z)G_{\lambda\beta}(0)$ operator, while another remains intact. In particular, the diagram 2a changes $G_{\mu\alpha}(z)$ into the sum of two terms. One of

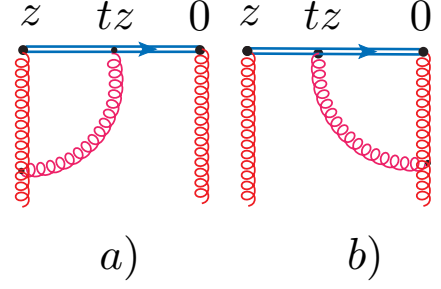


Figure 2: Vertex diagrams with gluons coming out of the gauge link.

them contains UV divergences, while the other one is UV finite.

The UV-divergent term is given by

$$\frac{N_c g^2}{4\pi^2} \frac{\Gamma(d/2-1)}{(d-2)(-z^2)^{d/2-1}} \int_0^1 du (u^{3-d} - u) \times (z_\alpha G_{z\mu}(\bar{u}z) - z_\mu G_{z\alpha}(\bar{u}z)), \quad (4.1)$$

where $G_{z\sigma} \equiv z^\rho G_{\rho\sigma}$ and $\bar{u} \equiv 1 - u$. The overall d -dependent factor here is finite for $d = 4$, but the u -integral diverges at the lower limit. Thus, just like in the case of the link self-energy diagram, the divergence appears in the integral over a dimensionless parameter t specifying the location of the endpoint of the gluon line on the gauge link. The divergence disappears if one uses the UV regularization by taking $d = 4 - 2\epsilon_{\text{UV}}$, which converts it into a pole at $\epsilon_{\text{UV}} = 0$.

Since the UV divergence comes from the $u \rightarrow 0$ integration, we can isolate it by taking $\bar{u} = 1$ in the gluonic field, which gives

$$\frac{N_c g^2}{4\pi^2} \frac{\Gamma(d/2-1)}{(d-2)(-z^2)^{d/2-1}} \left(\frac{1}{4-d} - \frac{1}{2} \right) \times (z_\alpha G_{z\mu}(z) - z_\mu G_{z\alpha}(z)). \quad (4.2)$$

The remainder is given by

$$\frac{N_c g^2}{4\pi^2} \frac{\Gamma(d/2-1)}{(d-2)(-z^2)^{d/2-1}} \int_0^1 du [u^{3-d} - u]_{+(0)} \times (z_\alpha G_{z\mu}(\bar{u}z) - z_\mu G_{z\alpha}(\bar{u}z)), \quad (4.3)$$

where the plus-prescription at $u = 0$ is defined as

$$\int_0^1 du [f(u)]_{+(0)} g(u) = \int_0^1 du f(u) [g(u) - g(0)]. \quad (4.4)$$

At first sight, the field $\mathcal{G}_{\mu\alpha}(z) = z_\alpha G_{z\mu}(z) - z_\mu G_{z\alpha}(z)$ accompanying the UV pole in Eq. (4.2) does not look like the field $G_{\mu\alpha}(z)$ in the original operator. Thus, one may worry that we are not dealing here with a multiplicative UV renormalization. So, let us perform an explicit check for our particular case when $z = \{0, 0, 0, z_3\}$.

To begin with, we see that $\mathcal{G}_{\mu\alpha}(z) = 0$ when both μ and α are transverse indices i, j . This corresponds

to a multiplicative renormalization with the anomalous dimension (AD) equal to zero.

Take now $\mu = 0$. Then $\mathcal{G}_{0\alpha}(z) = z_\alpha G_{z0}(z)$, so that $\mathcal{G}_{0i}(z) = 0$ while $\mathcal{G}_{03}(z) = -z_3^2 G_{30}(z) = z_3^2 G_{03}(z)$. Finally, if $\mu = 3$, then $\mathcal{G}_{3\alpha}(z) = -z_3 G_{z\alpha}(z) = z_3^2 G_{3\alpha}(z)$, which gives $\mathcal{G}_{3i}(z) = z_3^2 G_{3i}(z)$ and $\mathcal{G}_{30}(z) = z_3^2 G_{30}(z)$ (same result as above).

Thus, for all the cases, $\mathcal{G}_{\mu\alpha}(z)$ is a multiple of $G_{\mu\alpha}(z)$. Namely, when one of the indices equals 3, we have a nontrivial anomalous dimension, since $\mathcal{G}_{3\alpha}(z) = -\mathcal{G}_{\alpha 3}(z) = z_3^2 G_{3\alpha}(z)$. In all other cases, we have a trivial (vanishing) AD, since $\mathcal{G}_{ij}(z) = 0$ and $\mathcal{G}_{0i}(z) = 0$.

As mentioned, the link self-energy diagram has both linear and logarithmic UV divergences, while the vertex diagrams have just logarithmic UV divergences. Adding the logarithmic UV divergence coming from the link self-energy to the UV divergences of the vertex diagrams, we find, in particular, that the matrix elements $M_{0i;i0}$ and $M_{ij;ij}$ have the logarithmic AD due to the link self-energy diagram only. Call it γ . Comparing overall factors in Eqs. (3.6) and (4.2), we conclude that $M_{3i;i3}$ has the logarithmic AD equal to 2γ and matrix elements $M_{0i;i3} \pm M_{3i;i0}$ have the logarithmic AD equal to $\frac{3}{2}\gamma$. In addition, all of these structures acquire at one loop the same factor due to the linear UV singularity.

4.2. Evolution term

Our calculations show that the second, UV finite term from the diagram 2a is given by

$$\frac{N_c g^2}{8\pi^2} \frac{\Gamma(d/2 - 2)}{(d-3)(-z^2)^{d/2-2}} \int_0^1 du [u^{3-d} - 1]_{+(0)} \times G_{\mu\alpha}(\bar{u}z) G_{\lambda\beta}(0). \quad (4.5)$$

Note that the gluonic operator in Eq. (4.5) has the same tensor structure as the original operator $G_{\mu\alpha}(z)G_{\beta\nu}(0)$ differing from it just by rescaling $z \rightarrow \bar{u}z$. There is no mixing with operators of a different type. The u -integral in this case does not diverge for $d = 4$, but the overall $\Gamma(d/2 - 2)$ factor has a pole $1/(d-4)$.

Formally, there is also a pole $1/(d-3)$, corresponding to a linear UV divergence. However, the singularity for $d = 3$ is eliminated by the $[u^{3-d} - 1]$ combination in the integrand. One may say that the linear divergences present in “ u^{3-d} ” and “ -1 ” parts cancel each other.

In the calculation of Refs.[31, 18] performed using the usual Feynman gauge, the linear singularities cancel between contributions of two different diagrams shown in Fig. 1 of Ref. [18]. In our calculation, based on the bF gauge, the sum of these diagrams is represented by just one vertex diagram, so that the cancellation occurs inside the contribution (4.5) of that diagram.

The remaining $1/(d-4)$ pole corresponds to a collinear divergence developed because all the propagators correspond to massless particles. Taking a nonzero gluon mass λ , one would get a finite result containing $K_0(\sqrt{-z^2}\lambda)$ (see, e.g., Ref. [23] for a discussion of the quark vertex diagram in a similar context).

Still, $K_0(\sqrt{-z^2}\lambda)$ is only finite as far as z^2 is finite. The IR cut-off does not eliminate the logarithmic singularity $\ln(-z^2\lambda^2)$ that $K_0(\sqrt{-z^2}\lambda)$ has on the light cone. In the $z = z_3$ case, z_3^2 works like an ultraviolet cut-off for this singularity. This may be contrasted with the UV divergent contributions, where the UV cut-off is provided by the Polyakov regularization parameter a (or lattice spacing a_L) while z_3^2 appears on the IR side of the relevant logarithm $\ln(z_3^2/a^2)$.

5. Box diagram

There is also a contribution given by the diagram in Fig. 3 containing a gluon exchange between two gluon lines. This diagram does not have UV divergences, but it has DGLAP $\ln z_3^2$ contributions. In contrast to the vertex diagrams, the original $G_{\mu\alpha}(z)G_{\nu\beta}(0)$ operator generates now a mixture of bilocal operators corresponding to various projections of $G_{\mu\alpha}(\bar{u}z)G_{\nu\beta}(0)$ onto the structures built from vectors p, z and the metric tensor g .

In particular, in the case of the original $\langle p|G_{0i}(z)G_{0i}(0)|p\rangle$ matrix element, the box diagram contribution is expressed through matrix elements of $\langle p|G_{0i}(uz)G_{0i}(0)|p\rangle$, $\langle p|G_{3i}(uz)G_{3i}(0)|p\rangle$, $\langle p|G_{30}(uz)G_{30}(0)|p\rangle$ and $\langle p|G_{ij}(uz)G_{ij}(0)|p\rangle$ types. All these matrix elements also appear in the box diagram if one starts with the $\langle p|G_{3i}(z)G_{3i}(0)|p\rangle$ matrix element. Thus, in both cases we have a complicated mixing of different types of operators.

The situation is simpler for matrix elements

$$M_{03}^\pm(z, p) \equiv \langle p|G_{0i}(z)G_{i3}(0) \pm G_{3i}(z)G_{i0}(0)|p\rangle. \quad (5.1)$$

Namely, for $M_{03}^+(z, p)$ (or $M_{03}^-(z, p)$) combination, the box diagram contribution is expressed through $M_{03}^+(uz, p)$ (or $M_{03}^-(uz, p)$) only. However,

$$M_{03}^- \equiv M_{0i;i3} - M_{3i;i0} = 2p_0 z_3 (\mathcal{M}_{pz} - \mathcal{M}_{zp}). \quad (5.2)$$

does not contain the twist-2 function \mathcal{M}_{pp} , and is of no interest. For $M_{03}^+(z, p)$, the box contribution is given by

$$\frac{N_c g^2 \Gamma(d/2 - 1)}{4\pi^2 (-z^2)^{d/2-2}} \int_0^1 du \left(\bar{u}u + \frac{2}{3}\bar{u}^3 \right) M_{03}^+(uz, p) + \frac{N_c g^2 \Gamma(d/2 - 2)}{4\pi^2 (-z^2)^{d/2-2}} \int_0^1 du [\bar{u}(1+u^2) - u] M_{03}^+(uz, p). \quad (5.3)$$

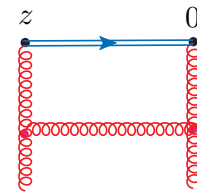


Figure 3: Box diagram.

Here, the $\Gamma(d/2 - 2)$ terms are singular for $d = 4$, which results in $\ln(-z^2)$ terms generating the DGLAP evolution. The $\Gamma(d/2 - 1)$ terms are singular for $d = 2$, which corresponds to the fact that the gluon propagator in two dimensions has a logarithmic $\ln(-z^2)$ behavior in the coordinate space. For $d = 4$, these terms are finite. Note that, unlike the vertex part, the box contribution does not have the plus-prescription form.

6. Gluon self-energy diagrams

One may expect that the plus-prescription form would appear after the addition of the gluon self-energy diagrams, one of which is shown in Fig. 4a. These diagrams have both the UV and collinear divergences. On the lattice, the UV divergence is regularized by the lattice spacing. In a continuum theory, one may use the Polyakov prescription $1/z^2 \rightarrow 1/(z^2 - a^2)$ for the gluon propagator. The collinear divergences may be regularized by taking a finite gluon mass λ . The result is a $\ln(a^2\lambda^2)$ contribution. However, it does not have the z -dependence, and apparently cannot help one to build the plus-prescription form for the $\ln z_3^2$ part of the box contribution.

A possible way out is to represent $\ln(a^2\lambda^2)$ as the difference $\ln(z_3^2\lambda^2) - \ln(z_3^2/a^2)$ of the evolution-type logarithm $\ln(z_3^2\lambda^2)$ and a UV-type logarithm $\ln(z_3^2/a^2)$. The latter can be added to the UV divergences of the diagrams 1 and 2 corresponding to link self-energy and vertex corrections. The $\ln(z_3^2\lambda^2)$ part is then added to the evolution kernel.

To be on safe side with gauge invariance, we use the dimensional regularization. Then the analog of the $\ln(a^2\lambda^2)$ logarithm is a pole $1/(2 - d/2)$ sometimes written as $1/\epsilon_{UV} - 1/\epsilon_{IR}$. For our purposes, it is more convenient to symbolically write it in a form similar to $\ln(a^2\lambda^2)$. Changing $\lambda \rightarrow \mu_{IR}$ and $a \rightarrow 1/\mu_{UV}$ we get $\ln(\mu_{IR}^2/\mu_{UV}^2)$, and then split this into the difference $\ln(z_3^2\mu_{IR}^2) - \ln(z_3^2\mu_{UV}^2)$.

We should also take into account the diagrams (one of them is shown in Fig. 4b) with an extra gluon line going out of the link-gluon vertex. The combined contribution of the Fig. 4 diagrams and their left-leg analogs is given by

$$\frac{g^2 N_c}{8\pi^2} \frac{1}{2 - d/2} \left[2 - \frac{\beta_0}{2N_c} \right] G_{\mu\alpha}(z) G_{\lambda\beta}(0), \quad (6.1)$$

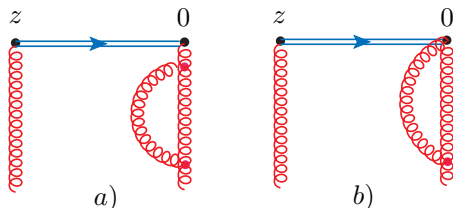


Figure 4: Gluon self-energy-type insertions into the right leg.

where $\beta_0 = 11N_c/3$ in gluodynamics, so that the terms in the square bracket combine into $1/6$. As discussed above, we will treat $1/(2 - d/2)$ as $\ln(z_3^2\mu_{IR}^2) - \ln(z_3^2\mu_{UV}^2)$.

7. DGLAP evolution structure

7.1. When DGLAP is diagonal in pure gluodynamics

The $M_{03}^+ \equiv M_{0i;i3} + M_{3i;i0}$ combination defined by Eq. (5.1) contains the twist-2 amplitude \mathcal{M}_{pp} ,

$$M_{03}^+ = 4p_0 p_3 \mathcal{M}_{pp} + 2p_0 z_3 (\mathcal{M}_{pz} + \mathcal{M}_{zp}), \quad (7.1)$$

though with a higher-twist admixture $\mathcal{M}_{zp} + \mathcal{M}_{pz}$. In the local limit, the relevant operator is proportional to the 3rd component of the Poynting vector

$$\mathbf{S}_3 = (\mathbf{E} \times \mathbf{B})_3 = E_1 B_2 - B_1 E_2 = -(G_{01} G_{13} + G_{32} G_{20}).$$

As already mentioned, the box part of the one-loop correction to the matrix element $M_{03}^+(z_3, p)$ in pure gluodynamics has a simple DGLAP structure¹ (5.3). Combining all the gluon one-loop corrections to it, we get, in the $\overline{\text{MS}}$ scheme,

$$\begin{aligned} & \frac{g^2 N_c}{8\pi^2} \int_0^1 du \left\{ \left[\left(\frac{3}{2} - \frac{1}{6} \right) \ln(z_3^2 \mu_{UV}^2 e^{2\gamma_E} / 4) + 2 \right] \delta(\bar{u}) \right. \\ & \quad \left. - 2 \log(z_3^2 \mu_{IR}^2 e^{2\gamma_E} / 4) \left[\frac{(1 - u\bar{u})^2}{\bar{u}} \right]_+ \right. \\ & \quad \left. + \left[u - 3 \frac{u}{\bar{u}} - 4 \frac{\log(\bar{u})}{\bar{u}} \right]_+ + 2 \left(\bar{u}u + \frac{2}{3} \bar{u}^3 \right) \right\} M_{03}^+(uz, p). \end{aligned} \quad (7.2)$$

The first line here comes from the UV-singular contributions. It contains the $\delta(\bar{u})$ factor which reflects the local nature of the UV divergences and converts $M_{03}^+(uz, p)$ into $M_{03}^+(z, p)$. The second line contains the Altarelli-Parisi (AP) kernel

$$B_{gg}(u) = 2 \left[\frac{(1 - u\bar{u})^2}{1 - u} \right]_+. \quad (7.3)$$

It has the plus-prescription structure reflecting the fact that, in the local limit, $\mathcal{M}_{pp}(z, p)$ is proportional to the matrix element of the gluon energy-momentum tensor. From now on, “+” means the plus-prescription at 1.

The third line contains z_3 -independent terms coming from the vertex diagrams (these have the plus-prescription form) and from the box diagram. The latter may be written as a sum of the term $2(\bar{u}u + \frac{2}{3}\bar{u}^3)_+$ that has the plus-prescription form and the term $\frac{2}{3}\delta(\bar{u})$ that may be combined with the UV terms.

7.2. Reduced Ioffe-time distribution

The combination $\mathcal{M}_{pz} + \mathcal{M}_{zp}$ is an odd function of $v = z_3 p_3$. Writing it as $2z_3 p_3 m_{zp}^+(v, z_3^2)$, we have

$$M_{03}^+(z_3, p) = 4p_3 p_0 [\mathcal{M}_{pp}(v, z_3^2) + z_3^2 m_{zp}^+(v, z_3^2)]. \quad (7.4)$$

¹This simplicity may be violated in higher orders.

Dividing out the kinematical factor $4p_3p_0$, we deal with

$$\widetilde{\mathcal{M}}_{pp}(\nu, z_3^2) \equiv \mathcal{M}_{pp}(\nu, z_3^2) + z_3^2 m_{zp}^+(\nu, z_3^2), \quad (7.5)$$

which is a function of ν and z_3^2 . Now, just like in the quark case considered in Refs. [10, 12], we can introduce the reduced Ioffe-time distribution

$$\widetilde{\mathfrak{M}}(\nu, z_3^2) \equiv \frac{\widetilde{\mathcal{M}}_{pp}(\nu, z_3^2)}{\widetilde{\mathcal{M}}_{pp}(0, z_3^2)}. \quad (7.6)$$

Since $\widetilde{\mathcal{M}}_{pp}(\nu, z_3^2)$ is obtained from the multiplicatively renormalizable combination M_{03}^+ , the UV divergent $Z(z_3^2\mu_{\text{IR}}^2)$ factors generated by the link-related and gluon self-energy diagrams cancel in the ratio (7.6). As a result, the small- z_3^2 dependence of the reduced pseudo-ITD $\widetilde{\mathfrak{M}}(\nu, z_3^2)$ comes from the logarithmic DGLAP evolution effects only. Moreover, $\widetilde{\mathcal{M}}_{pp}(0, z_3^2)$ has no DGLAP logarithmic dependence on z_3^2 , because of the plus-prescription nature of the AP kernel $B_{gg}(u)$.

Thus, neglecting $\mathcal{O}(z_3^2)$ terms, we conclude that, *in pure gluodynamics*, $\widetilde{\mathfrak{M}}(\nu, z_3^2)$ satisfies the evolution equation

$$\frac{d}{d \ln z_3^2} \widetilde{\mathfrak{M}}(\nu, z_3^2) = -\frac{\alpha_s}{2\pi} N_c \int_0^1 du B_{gg}(u) \widetilde{\mathfrak{M}}(u\nu, z_3^2) \quad (7.7)$$

with respect to z_3^2 . This relation is modified when gluon-quark transitions are present.

7.3. Gluon-quark mixing

In the $\overline{\text{MS}}$ scheme, the contribution to M_{03}^+ from the gluon-quark diagram shown in Fig. 5 is given by

$$\frac{g^2 C_F}{4\pi^2 z_3} \int_0^1 du \left[-2u - \ln(z_3^2 \mu_{\text{IR}}^2 e^{2\gamma_E} / 4) [2\bar{u} + \delta(\bar{u})] \right] \mathcal{O}_q(uz_3), \quad (7.8)$$

where $\mathcal{O}_q(z_3)$ is a singlet combination of quark fields,

$$\mathcal{O}_q(z_3) = \frac{i}{2} \sum_f \left(\bar{\psi}_f(0) \gamma_0 \psi_f(z_3) - \bar{\psi}_f(z_3) \gamma_0 \psi_f(0) \right), \quad (7.9)$$

with f numerating quark flavors. Note that $\mathcal{O}_q(z_3)$ vanishes for $z_3 = 0$. Expanding $\mathcal{O}_q(z_3)$ in z_3

$$\mathcal{O}_q(z_3) = z_3 \frac{i}{2} \sum_f \bar{\psi}_f(0) \gamma_0 \overleftrightarrow{\partial}_3 \psi_f(0) + \mathcal{O}(z_3^3), \quad (7.10)$$

we see that the lowest term is proportional to the quark part of the energy-momentum tensor. This term is accompanied by the z_3 factor which cancels the overall $1/z_3$ factor in Eq. (7.8).

The matrix element of $\mathcal{O}_q(z_3)$ can be parametrized by

$$\langle p | \mathcal{O}_q(z_3) | p \rangle = 2p^0 \int_0^1 dx \sin(xp_3 z_3) q_S(x) \quad (7.11)$$

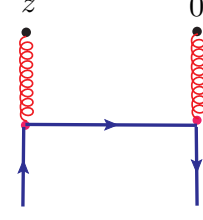


Figure 5: Gluon-quark mixing diagram.

where $f_S(x) = \sum_f [q_f(x) + \bar{q}_f(x)]$ is the singlet quark distribution. To extract the overall z_3 factor, we rewrite

$$\langle p | \mathcal{O}_q(z_3) | p \rangle = 2p^0 p_3 z_3 \int_0^1 dy \int_0^1 d\alpha \cos(\alpha y \nu) y f_S(y) \quad (7.12)$$

where $\nu = p_3 z_3$, as usual. This gives

$$\begin{aligned} & \frac{1}{z_3} \int_0^1 du A(u) \langle p | \mathcal{O}_q(uz_3) | p \rangle \\ & = 2p^0 p_3 \int_0^1 dw \mathcal{I}_S(w\nu) \mathcal{A}(w) \end{aligned} \quad (7.13)$$

for u -integrals of Eq. (7.8) type. Here

$$\mathcal{I}_S(\nu) = \int_0^1 dy \cos(y\nu) y f_S(y) \quad (7.14)$$

is the singlet quark Ioffe-time distribution, and

$$\mathcal{A}(w) = \int_w^1 du A(u). \quad (7.15)$$

For the evolution kernel $B_{gq}(u) \equiv 2\bar{u} + \delta(\bar{u})$, we get

$$\mathcal{B}_{gq}(w) = \int_w^1 du B_{gq}(u) = 1 + (1-w)^2. \quad (7.16)$$

7.4. Matching relations

A disadvantage of the $M_{03}^+(z_3, p)$ combination is that it vanishes when $p_3 = 0$ (see Eq. (7.4)). Thus, to extract $\widetilde{\mathcal{M}}_{pp}(\nu, z_3^2)$ for $\nu = 0$, one should make measurements of $M_{03}^+(z_3, p)$ for a few low values of p_3 , divide p_3 out, and extrapolate the results to $p_3 = 0$. This procedure leads to additional systematic uncertainties.

Fortunately, the combination $M_{0i;i0} - M_{ij;ij} = 2p_0^2 \mathcal{M}_{pp}$ of Eq. (2.12), being proportional to p_0^2 , does not have this problem. Furthermore, it gives the twist-2 amplitude \mathcal{M}_{pp} without contaminations. The amplitude $\mathcal{M}_{pp}(\nu, z_3^2)$ obtained in this way may be used to form the reduced pseudo-ITD $\widetilde{\mathfrak{M}}(\nu, z_3^2)$, as in Eq. (7.6).

Using the results of our calculations for the one-loop corrections to $M_{0i;i0}$ and $M_{ij;ij}$, and keeping just the \mathcal{M}_{pp} term in the correction (while skipping the ‘‘higher twist’’ terms $\mathcal{M}_{zz}, \mathcal{M}_{zp}, \mathcal{M}_{pz}, \mathcal{M}_{ppzz}$) we obtain

the matching relation

$$\begin{aligned} \mathfrak{M}(v, z_3^2) \mathcal{I}_g(0, \mu^2) &= \mathcal{I}_g(v, \mu^2) - \frac{\alpha_s N_c}{2\pi} \int_0^1 du \mathcal{I}_g(uv, \mu^2) \\ &\times \left\{ \ln(z_3^2 \mu^2 e^{2\gamma_E} / 4) B_{gg}(u) + 4 \left[\frac{u + \log(\bar{u})}{\bar{u}} \right]_+ \right. \\ &+ \left. \frac{2}{3} [1 - u^3]_+ \right\} - \frac{\alpha_s C_F}{2\pi} \ln(z_3^2 \mu^2 e^{2\gamma_E} / 4) \\ &\times \int_0^1 dw [\mathcal{I}_S(wv, \mu^2) - \mathcal{I}_S(0, \mu^2)] \mathcal{B}_{gq}(w) \quad (7.17) \end{aligned}$$

between the ‘‘lattice function’’ $\mathfrak{M}(v, z_3^2)$ and the light-cone ITDs $\mathcal{I}_g(v, \mu^2)$ and $\mathcal{I}_S(v, \mu^2)$. The first of them is related to the gluon PDF $f_g(x, \mu^2)$ by

$$\mathcal{I}_g(v, \mu^2) = \frac{1}{2} \int_{-1}^1 dx e^{ixv} x f_g(x, \mu^2). \quad (7.18)$$

Since $x f_g(x, \mu^2)$ is an even function of x , the real part of $\mathcal{I}_g(v, \mu^2)$ is given by the cosine transform of $x f_g(x, \mu^2)$, while its imaginary part vanishes. The factor $\mathcal{I}_g(0, \mu^2)$ has the meaning of the fraction of the hadron momentum carried by the gluons, $\mathcal{I}_g(0, \mu^2) = \langle x \rangle_{\mu^2}$.

Thus, Eq. (7.17) allows to extract the shape of the gluon distribution. Its normalization, i.e., the value of $\langle x \rangle_{\mu^2}$ should be found by an independent lattice calculation, similar to that performed in Ref. [39]. The singlet quark function $\mathcal{I}_S(wv, \mu^2)$ that appears in the $\mathcal{O}(\alpha_s)$ correction should be also calculated (or estimated) independently.

Substituting Eq. (7.18) into the matching condition (7.17), we can rewrite the latter in the kernel form [26]

$$\begin{aligned} \mathfrak{M}(v, z_3^2) &= \int_0^1 dx \frac{x f_g(x, \mu^2)}{\langle x \rangle_{\mu^2}} R_{gg}(xv, z_3^2 \mu^2) \\ &+ \int_0^1 dx \frac{x f_S(x, \mu^2)}{\langle x \rangle_{\mu^2}} R_{gq}(xv, z_3^2 \mu^2), \quad (7.19) \end{aligned}$$

where the kernel $R_{gg}(xv, z_3^2 \mu^2)$ is given by

$$\begin{aligned} R_{gg}(y, z_3^2 \mu^2) &= \cos y - \frac{\alpha_s}{2\pi} N_c \left\{ \ln \left(z_3^2 \mu^2 \frac{e^{2\gamma_E+2}}{4} \right) R_B(y) \right. \\ &+ \left. R_U(y) + R_L(y) + R_C(y) \right\}, \quad (7.20) \end{aligned}$$

with $R_B(y)$ being the cosine Fourier transform of the B_{gg} kernel

$$R_B(y) = \int_0^1 du B_{gg}(u) \cos(uy). \quad (7.21)$$

Its calculation is straightforward, and the result is expressed in terms of $\cos y$, $\sin y$ and the integral cosine $\text{Ci}(y)$ and sine $\text{Si}(y)$ functions. The latter come from the

$1/(1-u)$ part of $B(u)$, which gives

$$\begin{aligned} \int_0^1 du \left[\frac{1}{1-u} \right]_+ \cos(uy) &= \sin(y) \text{Si}(y) \\ &+ \cos(y) [\text{Ci}(y) - \log(y) - \gamma_E]. \quad (7.22) \end{aligned}$$

This combination also appears in $R_U(y)$, which is given by the cosine transform of $4[u/\bar{u}]_+$. Similarly, $R_L(y)$ is the cosine transform of the $4[(\ln \bar{u})/\bar{u}]_+$ term. It involves a hypergeometric function

$$R_L(y) = 4 \text{Re} \left[iy e^{iy} {}_3F_3(1, 1, 1; 2, 2, 2; -iy) \right]. \quad (7.23)$$

The $R_C(y)$ and $R_{gq}(y)$ kernels are given by the cosine transforms of $\frac{2}{3}[1-u^3]_+$ and $[1+\bar{u}^2]_+$, respectively. Expressions for them involve $\cos y$, $\sin y$ and inverse powers of y .

The important point is that the $R(y, z_3^2 \mu^2)$ kernels are given by *explicit* perturbatively calculable expressions. Using them and Eq. (7.19) one may directly relate $\mathfrak{M}(v, z_3^2)$ and the light-cone PDFs. Then, assuming some parameterizations for the $f_g(x, \mu^2)$ and $f_S(x, \mu^2)$ distributions, one can fit their parameters and α_s from the lattice data for $\mathfrak{M}(v, z_3^2)$ using Eqs. (7.19), (7.20). This procedure is essentially the same as that used in the ‘‘good lattice cross sections’’ approach [6, 7].

7.5. Matching relations for quasi-PDFs

The kernel relation (7.19) directly connects $\mathfrak{M}(v, z_3^2)$ with PDFs. So, there is no need to introduce intermediate functions, such as quasi-PDFs. Still, our results for particular matrix elements, such as Eq. (7.2) for $M_{03}^+(z_3, p)$, may be used to get matching conditions for quasi-PDFs. The latter are generically defined [4] as

$$Q(y, p_3) = \frac{p_3}{2\pi} \int_{-\infty}^{\infty} dz_3 \mathcal{M}(z_3, p) e^{-iy p_3 z_3}. \quad (7.24)$$

To proceed, one should write the amplitudes $\mathcal{M}(z_3, p)$ through the kernel relation (7.19) with $R(xv, z_3^2 \mu^2)$ expressed in terms of p_3 and z_3 , call it $J(x, p_3, z_3)$. The structure of its dependence on z_3 at one loop may be read off Eq. (7.2). For the gg part,

$$\begin{aligned} J_1^{gg}(x, p_3, z_3) &= (\gamma_U \ln z_3^2 + C_U) e^{ix p_3 z_3} \\ &- \int_0^1 du \left[\ln z_3^2 B_{gg}(u) + C(u) \right] e^{iux p_3 z_3}. \quad (7.25) \end{aligned}$$

The 1-loop quasi-PDF matching kernel is then given by

$$Z_1^{gg}(y, x, p_3) = \frac{p_3}{2\pi} \int_{-\infty}^{\infty} dz_3 J_1^{gg}(x, p_3, z_3) e^{-iy p_3 z_3}. \quad (7.26)$$

The C_U and $C(u)$ contributions of $J_1^{gg}(x, p_3, z_3)$ produce $C_U \delta(y-x)$ and $C(u) \delta(y-ux)$ terms. Hence, the resulting parts of $Q(y, p_3)$ are visible in the ‘‘canonical’’ $0 \leq |y| \leq 1$ region only. However, the terms with $\ln z_3^2$ give nonzero contributions in the $y/x > 1$ and $y/x < 0$

regions as well, namely

$$Z_1^{gg}(y, x, p_3)|_{y/x>1} = \frac{1}{|x|} \left[-\frac{\gamma_U}{\eta-1} + \int_0^1 du \frac{B_{gg}(u)}{\eta-u} \right], \quad (7.27)$$

where $\eta = y/x$. The $Z_1^{gg}(y, x, p_3)|_{y/x<0}$ term is given by the same expression, but with the opposite sign. Note that these contributions are completely determined by the AP kernel $B_{gg}(u)$ and the UV constant γ_U . Knowing them, one derives from Eq. (7.27) a general constraint on the results for $Z_1^{gg}(\eta, 1, p_3)|_{\eta>1}$ and $Z_1^{gg}(\eta, 1, p_3)|_{\eta<0}$ obtained by any Feynman diagram calculation. Using explicit form of $B_{gg}(u)$, we find

$$\int_0^1 du \frac{B_{gg}(u)}{\eta-u} = 2 \frac{(1-\eta\bar{\eta})^2}{\eta-1} \ln \frac{\eta-1}{\eta} + \frac{11}{6} \frac{1}{\eta-1} + \eta(2\eta-1) + \frac{11}{3}. \quad (7.28)$$

For large η , this expression tends to zero as $O(1/\eta^2)$. It should be stressed that such a behavior results from any kernel $B(u)$ that has the plus-prescription form.

This observation and the explicit expression given by Eq. (7.28) may be used to check the gluon-gluon matching kernels in Refs. [17, 18]. Our check shows that $Z_1^{gg}(y, 1, p_3)|_{y>1}$ corresponding to Eq. (64) of Ref. [18] does not satisfy the constraint (7.27). The difference is by a constant term ($-2/3$) that leads to a linear divergence in the integral of $Z_1^{gg}(y, 1, p_3)|_{y>1}$ over y . The same difference (with the opposite sign) appears in the $Z_1^{gg}(y, 1, p_3)|_{y<0}$ term in Eq. (64) of Ref. [18]. Apparently, these differences result from the use of the off-shell external gluon fields in the calculations of Ref. [18], but a discussion of this topic is outside of the scope of our paper.

8. Summary.

In this paper, we have presented the results that form the basis for the ongoing efforts to calculate gluon PDF using the pseudo-PDF approach.

In particular, we gave a classification of possible two-gluon correlator functions. We have identified those of them that contain the invariant amplitude $\mathcal{M}_{pp}(\nu, -z^2)$ that determines the gluon PDF in the light-cone $z^2 \rightarrow 0$ limit. Since this limit is singular, one needs the matching conditions that relate $\mathcal{M}_{pp}(\nu, z_3^2)$ to the light-cone PDF $f(x, \mu^2)$.

To this end, using the method of Ref. [27], we have performed calculations of the one-loop corrections to the gauge-invariant correlator of two gluon field-strength tensors, with all Lorentz indices explicit. To preserve gauge invariance, we have used the dimensional regularization.

Since the DR produces the same form $\ln z_3^2 \mu^2$ both for logarithms related to the UV singularities and for those reflecting the DGLAP evolution, we have made an effort to separate these two sources of the

$\ln z_3^2$ -dependence at small z_3^2 . When we form a reduced ITD $\mathfrak{R}(\nu, z_3^2)$, the UV-related contributions are canceled, and only the DGLAP-related terms remain in the matching relation between the reduced ITD and the light-cone ITD.

The matching relation may be also written in a kernel form (7.19) that directly connects lattice data on $\mathfrak{R}(\nu, z_3^2)$ with the normalized gluon PDF $x f_g(x, \mu^2)/\langle x \rangle_{\mu^2}$. The average gluon momentum fraction $\langle x \rangle_{\mu^2}$ needs to be extracted from a separate lattice calculation.

We have also demonstrated that our results may be used for a rather straightforward calculation of the one-loop corrections to quasi-PDFs, providing new insights concerning their structure that may be used to check the results for the gluon quasi-PDF matching conditions.

In a future publication, we plan to present more details of our calculations, and to give a complete result for the box diagram, in particular for the non-forward kinematics that are needed in lattice calculations of distribution amplitudes and GPDs. We also plan to include calculations for gluon-quark and quark-gluon terms.

Acknowledgements. We thank K. Orginos, J.-W. Qiu, D. Richards and S. Zhao for interest in our work and discussions. This work is supported by Jefferson Science Associates, LLC under U.S. DOE Contract #DE-AC05-06OR23177 and by U.S. DOE Grant #DE-FG02-97ER41028.

References

- [1] K. Cichy and M. Constantinou, *Adv. High Energy Phys.* **2019** (2019) 3036904
- [2] W. Detmold and C. J. D. Lin, *Phys. Rev. D* **73** (2006) 014501
- [3] V. Braun and D. Müller, *Eur. Phys. J. C* **55** (2008) 349
- [4] X. Ji, *Phys. Rev. Lett.* **110** (2013) 262002
- [5] X. Ji, *Sci. China Phys. Mech. Astron.* **57** (2014) 1407
- [6] Y. Q. Ma and J. W. Qiu, *Phys. Rev. D* **98** (2018) no.7, 074021
- [7] Y. Q. Ma and J. W. Qiu, *Phys. Rev. Lett.* **120** (2018) no.2, 022003
- [8] G. S. Bali *et al.*, *Eur. Phys. J. C* **78** (2018) no.3, 217
- [9] G. S. Bali *et al.*, *Phys. Rev. D* **98** (2018) no.9, 094507
- [10] A. V. Radyushkin, *Phys. Rev. D* **96** (2017) no.3, 034025
- [11] A. Radyushkin, *PoS QCDEV 2017* (2017) 021
- [12] K. Orginos, A. Radyushkin, J. Karpie and S. Zafeiropoulos, *Phys. Rev. D* **96** (2017) no.9, 094503
- [13] X. Xiong, X. Ji, J. H. Zhang and Y. Zhao, *Phys. Rev. D* **90** (2014) no.1, 014051
- [14] X. Ji and J. H. Zhang, *Phys. Rev. D* **92** (2015) 034006
- [15] T. Izubuchi, X. Ji, L. Jin, I. W. Stewart and Y. Zhao, *Phys. Rev. D* **98** (2018) no.5, 056004
- [16] W. Wang and S. Zhao, *JHEP* **1805** (2018) 142
- [17] W. Wang, S. Zhao and R. Zhu, *Eur. Phys. J. C* **78** (2018) no.2, 147
- [18] W. Wang, J. H. Zhang, S. Zhao and R. Zhu, arXiv:1904.00978 [hep-ph].
- [19] X. Ji, A. Schäfer, X. Xiong and J. H. Zhang, *Phys. Rev. D* **92** (2015) 014039
- [20] X. Xiong and J. H. Zhang, *Phys. Rev. D* **92** (2015) no.5, 054037
- [21] Y. S. Liu, W. Wang, J. Xu, Q. A. Zhang, J. H. Zhang, S. Zhao and Y. Zhao, *Phys. Rev. D* **100** (2019) no.3, 034006
- [22] X. Ji, J. H. Zhang and Y. Zhao, *Nucl. Phys. B* **924** (2017) 366
- [23] A. V. Radyushkin, *Phys. Lett. B* **781** (2018) 433
- [24] A. Radyushkin, *Phys. Rev. D* **98** (2018) no.1, 014019
- [25] J. H. Zhang, J. W. Chen and C. Monahan, *Phys. Rev. D* **97** (2018) no.7, 074508

- [26] A. V. Radyushkin, Phys. Rev. D **100** (2019) no.11, 116011
- [27] I. I. Balitsky and V. M. Braun, Nucl. Phys. B **311** (1989) 541.
- [28] B. L. Ioffe, Phys. Lett. **30B**, 123 (1969)
- [29] G. Altarelli and G. Parisi, Nucl. Phys. B **126** (1977) 298.
- [30] Z. Y. Li, Y. Q. Ma and J. W. Qiu, Phys. Rev. Lett. **122** (2019) no.6, 062002
- [31] J. H. Zhang, X. Ji, A. Schäfer, W. Wang and S. Zhao, Phys. Rev. Lett. **122** (2019) no.14, 142001
- [32] Z. Y. Fan, Y. B. Yang, A. Anthony, H. W. Lin and K. F. Liu, Phys. Rev. Lett. **121** (2018) no.24, 242001
- [33] V. N. Gribov and L. N. Lipatov, Sov. J. Nucl. Phys. **15** (1972) 438 [Yad. Fiz. **15** (1972) 781].
- [34] Y. L. Dokshitzer, Sov. Phys. JETP **46** (1977) 641 [Zh. Eksp. Teor. Fiz. **73** (1977) 1216].
- [35] G. 't Hooft and M. J. G. Veltman, Nucl. Phys. B **44** (1972) 189
- [36] A. M. Polyakov, Nucl. Phys. B **164** (1980) 171.
- [37] J. W. Chen, X. Ji and J. H. Zhang, Nucl. Phys. B **915** (2017) 1
- [38] L. F. Abbott, Nucl. Phys. B **185** (1981) 189.
- [39] Y. B. Yang, M. Gong, J. Liang, H. W. Lin, K. F. Liu, D. Pefkou and P. Shanahan, Phys. Rev. D **98** (2018) no.7, 074506